Molecular and Cellular Neuroscience 41 (2009) 409–419

Contents lists available at ScienceDirect

Molecular and Cellular Neuroscience

journal homepage: www.elsevier.com/locate/ymcne

A central role for the small GTPase Rac1 in hippocampal plasticity and spatial learning and memory

Ursula Haditsch [a,*], Dino P. Leone [b], Mélissa Farinelli [c], Anna Chrostek-Grashoff [d,e], Cord Brakebusch [d], Isabelle M. Mansuy [c], Susan K. McConnell [b], Theo D. Palmer [a,*]

[a] Department of Neurosurgery, Stanford School of Medicine, 1201 Welch Rd, MSLS P304, Stanford, California, 94305, USA
[b] Department of Biology, Stanford University, Stanford, California, USA
[c] Brain Research Institute, University of Zürich, Zürich, Switzerland
[d] Biotech Research and Innovation Centre, University of Copenhagen, Copenhagen, Denmark
[e] Cardiovascular Research Center, University of Virginia Health System, Charlottesville, Virginia, USA

ARTICLE INFO

Article history:
Received 22 September 2008
Revised 17 April 2009
Accepted 17 April 2009
Available online 24 April 2009

ABSTRACT

Rac1 is a member of the Rho family of small GTPases that are important for structural aspects of the mature neuronal synapse including basal spine density and shape, activity-dependent spine enlargement, and AMPA receptor clustering *in vitro*. Here we demonstrate that selective elimination of Rac1 in excitatory neurons in the forebrain *in vivo* not only affects spine structure, but also impairs synaptic plasticity in the hippocampus with consequent defects in hippocampus-dependent spatial learning. Furthermore, Rac1 mutants display deficits in working/episodic-like memory in the delayed matching-to-place (DMP) task suggesting that Rac1 is a central regulator of rapid encoding of novel spatial information *in vivo*.

Introduction

Plasticity in the brain enables us to respond to changes in the environment by learning and remembering. Many forms of neural pathology are accompanied by altered plasticity, thus it is important to understand the molecular mechanisms that regulate experience-dependent alterations in neural function. In the adult hippocampus, rapid experience-dependent plasticity is mediated by alterations in the strengths of individual synapses. Long-term potentiation (LTP), a well-characterized form of synaptic plasticity, is accompanied by rapid changes in both synapse size and number (Geinisman, 2000; Harris et al., 2003).

Changes in synapse size and number require a dynamic actin cytoskeleton (Bonhoeffer and Yuste, 2002; Calabrese et al., 2006; Dillon and Goda, 2005), and one of the best-characterized pathways for regulation of actin dynamics involves the Rho family of small GTPases, Rac1, Cdc42 and Rho (Hall, 1998, 2005). Rac1 and Cdc42 regulate actin polymerization through several pathways, one of which involves the activation of the p21-activated kinases PAK 1, 2 and 3, which in turn phosphorylate and activate the LIM-domain-containing protein kinase 1 (LIMK1) (Bokoch, 2003; Edwards et al., 1999). Once active, LIMK1 phosphorylates and inhibits cofilin, an actin filament depolymerizing/severing factor, thus stabilizing actin filaments and promoting actin polymerization (Bamburg, 1999; Stanyon and Bernard, 1999).

Many forms of mental retardation have been linked to mutations affecting Rho GTPase signaling cascades and are associated with alterations in the morphology and density of dendritic spines. Mutations in the X-linked mental retardation disease genes *OPHN1* and α*PIX*, which encode a guanine nucleotide exchange factor (GEF) and a GTPase activation protein (GAP), respectively, are associated with abnormalities in dendritic spines in the hippocampus (van Galen and Ramakers, 2005). GEFs mediate the exchange of GDP for GTP, thereby activating Rho GTPases; GAPs, on the other hand, increase the endogenous GTPase activity of Rho GTPases, thus facilitating a switch to the "off" state. Rac1 activation in spines is regulated by different GEFs such as α- and βPIX, Tiam1 and kalirin-7, which are activated downstream of the NMDA receptor, the EphB receptor and TrkB receptor (Miyamoto et al., 2006; Penzes et al., 2003; Saneyoshi et al., 2008; Tolias et al., 2005; Tolias et al., 2007; Xie et al., 2007).

In vitro studies have shown that Rac1 activity plays an essential role in activity-dependent spine enlargement and AMPA receptor clustering during synapse maturation (Tashiro et al., 2000; Tashiro and Yuste, 2004; Wiens et al., 2005). Furthermore, overexpression of a dominant-negative Rac1 decreases the number of spines and synapses in hippocampal cultures and slices (Nakayama et al., 2000; Zhang et al., 2003). Although these studies strongly implicate Rac1 in experience-induced plasticity, there are no studies that have directly tested whether neuronal Rac1 is necessary for experience-dependent plasticity and normal learning and memory function in intact animals. Gain of function experiments have shown that expression of

* Corresponding authors.
E-mail addresses: ursula.haditsch@stanford.edu (U. Haditsch), tpalmer@stanford.edu (T.D. Palmer).

1044-7431/$ – see front matter © 2009 Elsevier Inc. All rights reserved.
doi:10.1016/j.mcn.2009.04.005

constitutively active human Rac1 in Purkinje cells alters spine morphology and number and causes ataxia in transgenic mice (Luo et al., 1996). Diana et al. (2007) have also suggested that activation of Rho GTPases in neurons can improve synaptic plasticity and learning and memory. However the drug used in the latter study, CNF1, not only activates Rac1, RhoA and Cdc42 but also induces a pronounced inflammatory response that leads to the production of monocyte chemotactic protein-1 (MCP-1), interleukin-8 (IL-8), IL-6, monocyte inflammatory protein-3 (MIP-3) and E-selectin (Munro et al., 2004). Thus it has been uncertain whether Rac1 alone is indeed important for cognitive functions that rely on plasticity.

Here we directly assess the role of Rac1 in neurons *in vivo* by conditionally ablating Rac1 in mature neurons in the forebrain and evaluating consequent changes in hippocampal plasticity and hippocampus-dependent learning and memory. We demonstrate that loss of Rac1 attenuates synapse structure and function *in vivo*, which ultimately leads to significant defects in spatial learning and working/episodic-like memory.

Results

Ablation of Rac1 in mature postmitotic neurons of the hippocampus

To ablate Rac1 function in mature pyramidal neurons of the hippocampus, we used the Cre-LoxP system to selectively excise *Rac1* coding sequences. Transgenic mice expressing the Cre recombinase

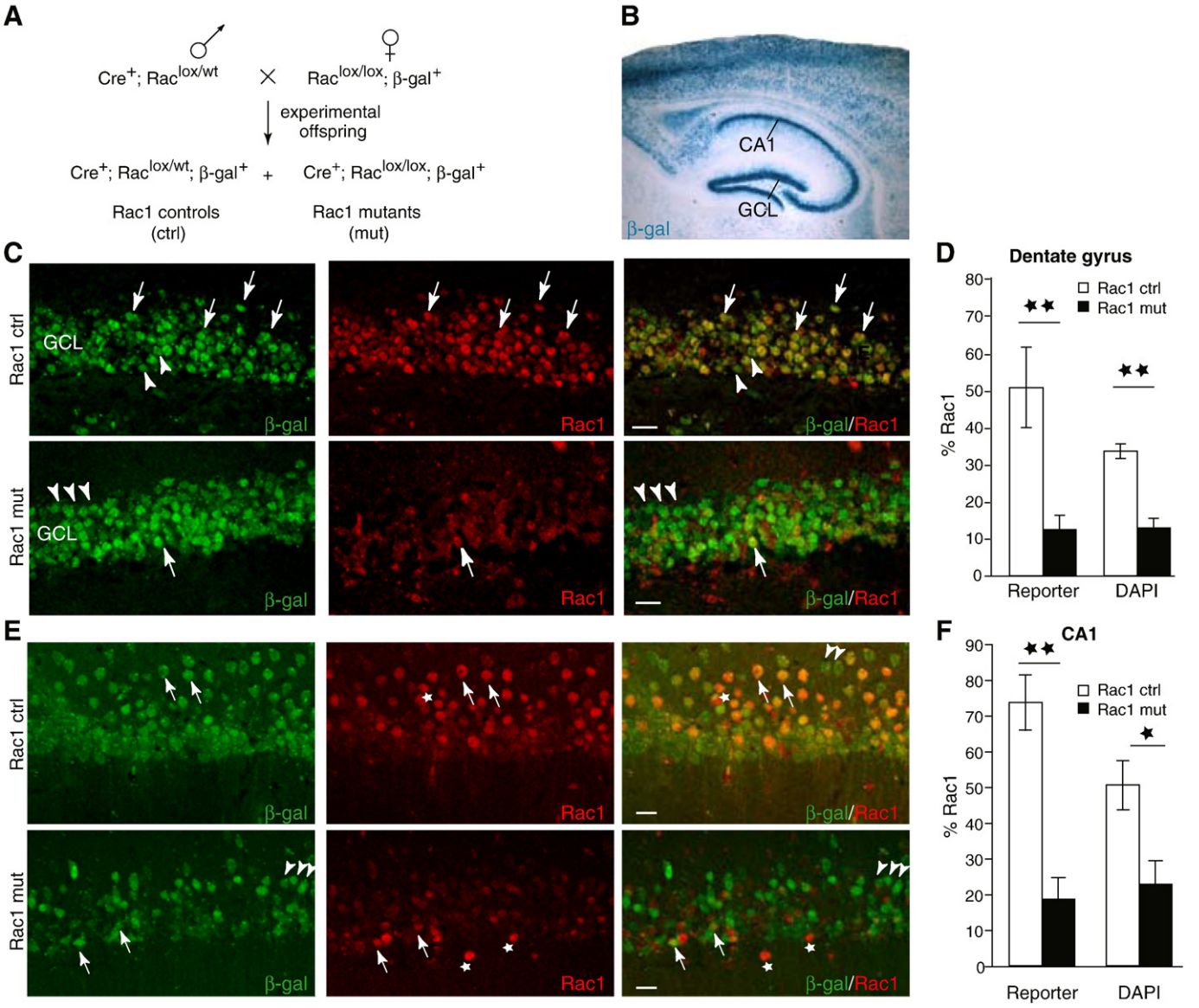

Fig. 1. Reporter and Rac1 expression in the hippocampus. (A) Animal mating strategy. To generate Rac1 controls and mutants, mice hemizygous for the CamKIIα-*cre* transgene and heterozygous for the floxed alleles (Cre^{+}; $Rac1^{lox/wt}$) were crossed to mice that were homozygous for the floxed alleles ($Rac1^{lox/lox}$) and carried either the R26R or the Z/EG reporter allele. (B) Xgal staining of an $R26R^{+}$ control mouse reveals β galactosidase (β-gal) expression in the granule cell layer (GCL) of the dentate gyrus (DG) and the pyramidal cell layer of the CA1 region. (C) Double staining of granular cells of the DG for β-gal and Rac1 in control (top panels) and mutant animals (lower panels). About half of the $\beta\text{-gal}^{+}$ cells co-expressed Rac1 in control mice (arrows); a smaller fraction of $\beta\text{-gal}^{+}$ cells lacked Rac1 expression (arrow heads). Scale bars = 20 μm. (D) Rac1 expression was significantly reduced in $reporter^{+}$ cells in the GCL (controls, $n=4$; mutants, $n=6$, ANOVA, $F_{1,8}=15.28$), and $DAPI^{+}$ cells in the GCL showed an overall reduction of Rac1 (controls, $n=11$; mutants, $n=7$, ANOVA, $F_{1,16}=39.7$). (E) Double staining of pyramidal neurons of the CA1 regions for β-gal and Rac1 in control (top panel) and mutant animals (lower panel). The majority of $\beta\text{-gal}^{+}$ cells co-express Rac1 in control mice (arrows); a smaller fraction of $\beta\text{-gal}^{+}$ cells lack Rac1 expression (arrowheads), and some cells express Rac1 but are β-gal negative (stars). In mutant mice, lower Rac1 expression is apparent. Scale bars = 20 μm. (F) Rac1 expression was significantly reduced in $reporter^{+}$ cells in CA1 (controls, $n=4$; mutants, $n=9$, ANOVA, $F_{1,11}=46.9$), and an overall reduction of Rac1 was observed in $DAPI^{+}$ pyramidal cells (controls, $n=11$; mutants, $n=10$, ANOVA, $F_{1,19}=14.7$). $^{*}p<0.05$, $^{**}p<0.01$.

under the control of the CamKIIα promoter (Schweizer et al., 2003) were crossed with mice carrying a conditional allele of Rac1 ($Rac1^{lox}$) (Chrostek et al., 2006). CamKII-Cre drives recombination in hippocampal pyramidal neurons and the granule neurons of the dentate gyrus (DG), as visualized by the Rosa26 reporter (Soriano, 1999) or the Z/EG allele (Novak et al., 2000), which express β-galactosidase (β-gal; Fig. 1B) or enhanced green fluorescent protein (EGFP, not shown), respectively, upon recombination. Immunostaining for Rac1 protein confirmed that control (Cre^{+};$Rac1^{lox/wt}$) mice showed extensive co-localization of Rac1 and β-gal in the granule cell layer (GCL) and CA1 regions of the hippocampus, and that co-localization was significantly reduced in Rac1-deficient (Cre^{+};$Rac1^{lox/lox}$) mice (Figs. 1C and E). Quantification revealed a significant reduction of Rac1 expression in the GCL and the CA1 regions in both reporter-positive cells and DAPI-positive cells (Figs. 1D and F), demonstrating that Cre-mediated excision resulted in an efficient reduction in the fraction of mature neurons expressing detectable levels of Rac1. The loss of Rac1 did not change the expression levels of the other Rho GTPases Cdc42 (Fig. S1) and RhoA (data not shown) in the hippocampus.

Rac1 regulates actin polymerization by triggering the phosphorylation and activation of PAK1 (Edwards et al., 1999); thus, to visualize ongoing Rac1 activity, we used a phospho-specific antibody against activated PAK 1–3 (P-PAK) to reveal P-PAK expression in hippocampal neurons. Control mice exhibited high levels of P-PAK staining in the pyramidal cell layer of CA1 (Fig. 2A) and the GCL (data not shown). In contrast, Rac1-deficient mice displayed significantly fewer P-PAK^{+} cells in both areas (Fig. 2B), consistent with the notion that loss of Rac1 alters actin dynamics in mutant neurons through PAK activity (Bokoch, 2003; Edwards et al., 1999).

Loss of Rac1 in vivo affects PSD-95 density and spine size

The consequences of deleting Rac1 in neurons were similar to those observed previously when a dominant-negative form of Rac1 was overexpressed in cultured hippocampal slices, which resulted in defects in synapse number and morphology (Nakayama et al., 2000). Following genetic deletion of *Rac1*, the $EGFP^{+}$ basal dendrites of CA1 neurons and $EGFP^{+}$ dendrites in the molecular layer of the granular neurons of the DG had a 19.7 ± 2.3% and 23.1 ± 2.9% reduction in PSD-95^{+} puncta, respectively, which mark postsynaptic densities (PSDs, Figs. 3A, B). Furthermore, the overall number of PSD-95^{+} clusters (regardless of EGFP co-localization) was reduced in both brain areas (Figs. S2A–C).

Electron microscopic analyses of spine morphology were performed for CA1 pyramidal neurons to evaluate PSD length, spine thickness, spine head area, and the distance between pre- and postsynaptic sites (cleft width, Fig. 3C). PSD length and spine head area are representative of spine volume and are thus useful in assessing changes in spine size (Luo et al., 1996). Spine thickness was not changed in Rac1 mutants (Fig. 3D). However, mean PSD length was significantly increased (Fig. 3E1) and mean spine head area (Fig. 3E2) was significantly larger in the mutant mice. Frequency distribution plots indicate that these differences were not due to the presence of a small subset of abnormally large spines (Figs. 3F1, F2, in both cases Kolmogorov–Smirnov test, $p>0.6$) but rather to an overall increase in length and area uniformly across all spine sizes. Finally, synaptic cleft widths also showed significant increases in mutant CA1 neurons compared to controls (Fig. 3G). Taken together, these results show that Rac1-deficient neurons have fewer synapses, but both the presynaptic spines and postsynaptic densities of existing spines are larger than those observed in control hippocampal neurons.

Loss of Rac1 impairs LTP in both CA1 and dentate gyrus

To determine whether Rac1-deficient mice show alterations in synaptic plasticity, we compared hippocampal LTP in acutely prepared slices of control and mutant brains. Excitatory postsynaptic potentials (fEPSPs) were measured in CA1 and DG neurons before and after the application of 3 trains of electrical stimulation at 100 Hz. Mutant neurons showed a severe impairment of LTP in both CA1 (control = 161.47 ± 4.0%, mutant = 123.24 ± 8.25%; ANOVA, $F_{1,16}=17.38$, $p<0.001$; Fig. 4A) and DG (control = 168.53 ± 8.36%, mutant = 127.09 ± 7.54%; ANOVA, $F_{1,17}=26.4$, $p<0.001$; Fig. 4B) regions. These deficits

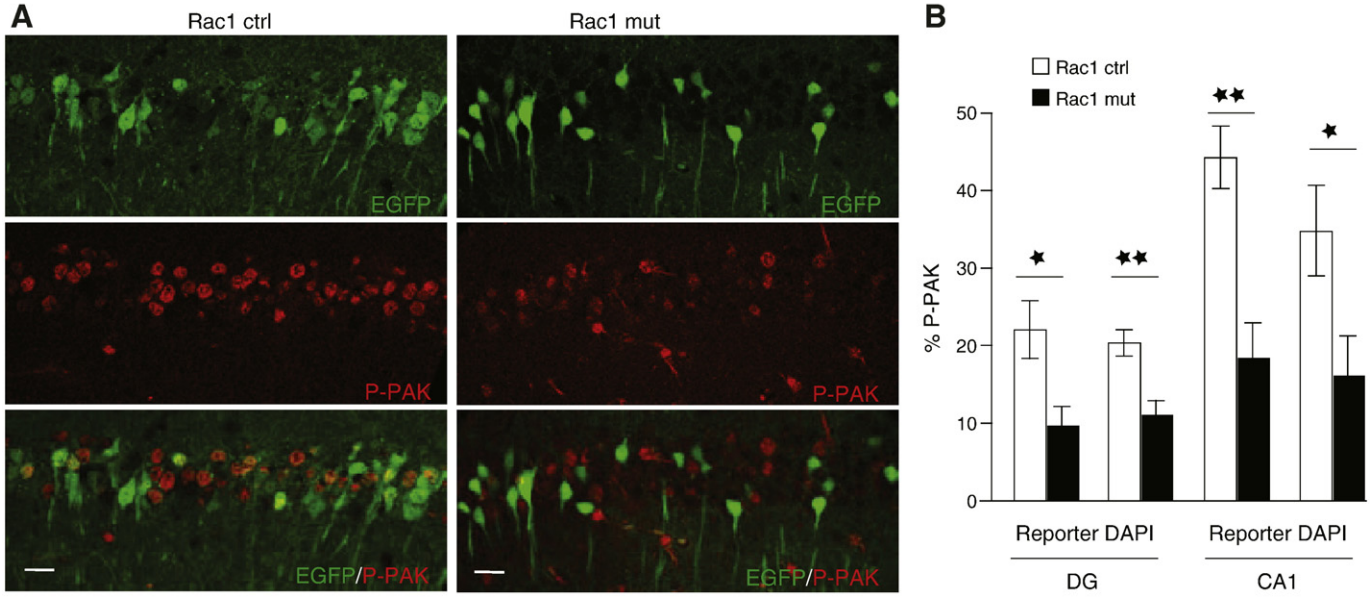

Fig. 2. P-PAK expression in the CA1 and DG regions of the hippocampus. (A) Immunostaining for phosphorylated p21-aktivated kinase (P-PAK, red) and EGFP reporter (green) in control (left panels) and mutant mice (right panels). Scale bar = 20 μm. (B) P-PAK expression was significantly reduced in the DG and the CA1 in reporter^{+} cells (DG, $n=3$ for both groups, ANOVA, $F_{1,5}=8.87$; CA1, controls, $n=3$, mutants = 6, ANOVA, $F_{1,7}=20.2$); P-PAK expression was also reduced in DAPI^{+} pyramidal cells (DG, controls = 7, mutants = 5, $F_{1,10}=15.4$; CA1, controls, $n=8$; mutants, $n=6$, $F_{1,12}=5.4$). *$p<0.05$, **$p<0.01$.

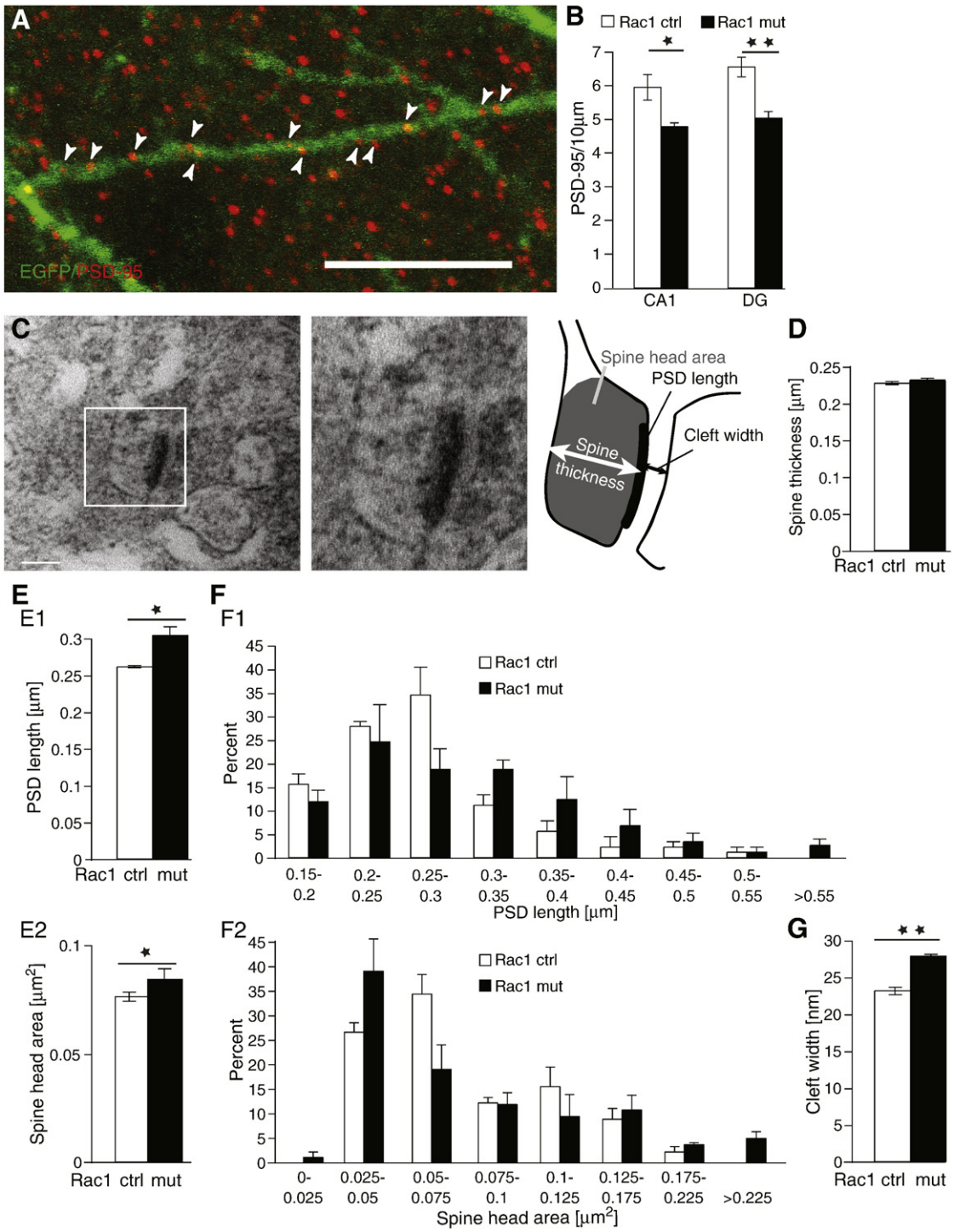

Fig. 3. PSD-95 densities and synapse size are altered in Rac1 mutants. (A) Co-localization of EGFP (green) with the postsynaptic density marker PSD-95 (red) in basal dendrites of CA1 neurons of a Rac1 control mouse. Scale bar = 10 µm. (B) Quantification of PSD-95$^+$ densities in the basal dendrites of CA1 neurons and in the granule cell dendrites in the molecular layer of the DG. Rac1 mutants showed a significant decrease in PSD-95$^+$ clusters in both areas (controls, $n=5$, mutants, $n=6$, ANOVA, CA1, $F_{1,9}=8.76$, $p<0.05$; DG, $F_{1,9}=20.25$, $p<0.01$). (C) Electron micrograph of an EGFP$^+$ synapses in the striatum radiatum of CA1. The schematic drawing on the right highlights the different parameters assessed. Scale bar = 0.2 µm. (D) No changes in spine thickness in Rac1 mutants. (E1) Mean PSD length was significantly longer in Rac1 mutants than in control mice ($n=3$ for all groups, ANOVA, $F_{1,4}=13.52$, $p<0.05$). (E2) Mean spine head area was significantly larger in the mutants, ($n=3$ for all groups, ANOVA, $F_{1,4}=9.02$, $p<0.05$). (F) Frequency distribution plots of PDS length (F1) and cross-sectional spine head area (F2) revealed no asymmetric changes in the distribution between Rac1 mutants and control mice in either measurement (in both cases Kolmogorov–Smirnov test, $p>0.5$). (G) Distance between pre- and postsynaptic site (cleft width) was longer ($n=3$ for all groups, ANOVA, $F_{1,4}=130.4$, $p<0.01$). *$p<0.05$, **$p<0.01$.

were not caused by general impairments of synaptic transmission since basal transmission was normal in both regions (Figs. 4C and D). The loss of Rac1 in mature hippocampal neurons thus affects both synapse structure and function.

Rac1-deficient mice have impaired spatial learning, but normal memory

To examine whether these structural and electrophysiological defects lead to deficits in learning and memory, we tested control and

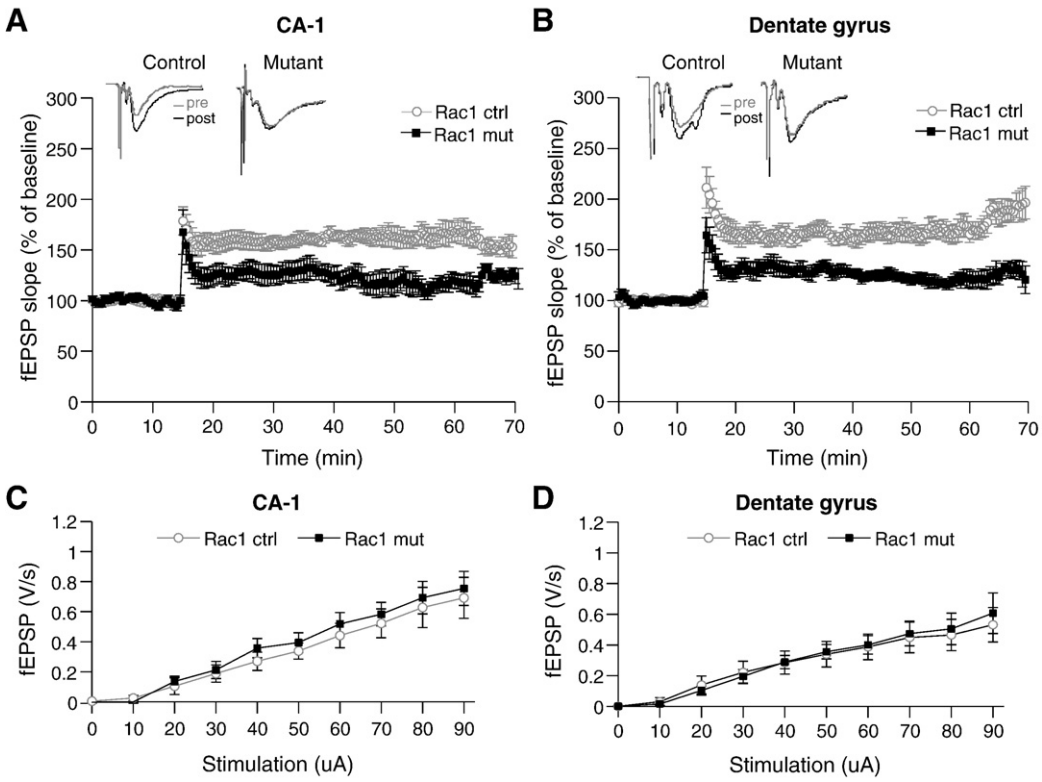

Fig. 4. LTP is impaired in Rac1 mutants. (A, B) LTP was elicited by three trains of 100-Hz stimulation in control ($n=9$) and mutant slices ($n=10$) in CA1 (A) and DG (B). Insets: Representative examples of evoked responses shown immediately before (pre) and 30 min after (post) induction of LTP. The stimulation induced normal LTP in control slices, but LTP was significantly diminished in mutant slices in both CA1 region (control = 161.47 ± 4.0%, mutant = 123.24 ± 8.25%; two-way repeated measures ANOVA, $F_{1,17}=17.38$, $p<0.001$) and DG (control = 168.53 ± 8.36%, mutant = 127.09 ± 7.54%; two-way repeated measures ANOVA, $F_{1,17}=26.4$, $p<0.001$). (C, D) Input–output curves of synaptic transmission in control and mutant slices. fEPSP in CA1 (A) and DG (B) regions revealed no difference in basal transmission between Rac1 mutant slices ($n=11$) and control littermates ($n=11$) (ANOVA, $p>0.7$).

mutant mice on the Morris water maze, a hippocampus-dependent task that is used to assess spatial learning and memory (Morris et al., 1982). Briefly, the animals must learn the location of a hidden platform by using external visual cues surrounding the pool. Both mutant and control groups readily learned the location of the hidden platform, as shown by a decrease in the escape latency (time to reach the platform; Fig. 5A). However, Rac1-deficient animals required significantly more time to locate the hidden platform as evidenced by significant longer escape latencies on several training days (days 1, 2 and 7) and an overall genotype effect measured over all days (two-way repeated measures ANOVA, $F_{1,24}=4.66$, $p<0.05$) suggests that learning was impaired in these mice.

After learning, memory was evaluated by a probe trial in which the platform was removed and the time each animal spends in the correct quadrant is measured. For each animal, memory was repeatedly assessed at specific retention intervals (including 1 day and 1, 2, 3, 4, and 5 weeks after the last training). No differences between Rac1 mutant and control animals were found, suggesting that Rac1-deficient mice did not experience memory deficits (Fig. 5B). Tests of reversal training, visible platform training and analysis of parameters such as swim distance (Figs. 5C–E) and thigmotaxis (data not shown) revealed no significant differences between controls and mutants. Taken together, these results suggest that the impaired performance in Rac1 mutants resulted from diminished hippocampus-dependent spatial learning and not from changes in motor, motivational, or emotional processes.

Rac1-deficient mice have impaired working/episodic-like memory

We next assessed whether working/episodic-like memory, which is an immediate and rapidly decaying memory, was impaired in mutant mice. Animals were tested in the "delayed matching-to-place" (DMP) version of the Morris water maze (Fig. 6A), a task that depends on the integrity of the hippocampus and NMDA receptor activation (Steele and Morris, 1999). To test visual acuity, the animals were first trained on the cued version of the task. No differences between control and mutant mice were observed in visual acuity (Fig. 6B) or swimming velocity (Fig. 6F). On the first day of the DMP task, mice were trained to navigate to a hidden platform at a fixed location in the water maze for 12 trials with 5 min intervals between each trial (Fig. 6A). Each following training day began in the same manner except that the platform was moved to a new location in the maze. Thus, after a total of 7 training days, 7 different hidden platform locations were learned sequentially. Finally, on days 8 and 9, the interval between each training trial was extended from 5 to 60 min with only 6 training trials per day. Both control and mutant mice showed learning across the 12 sessions within each training day. However, control mice reduced their escape latency at a much faster rate than Rac1-deficient mice. Overall, there was a significant difference between genotypes across the first seven days (Fig. 6C; three-way repeated measures ANOVA, $F_{1,23}=9.96$, $p<0.01$), as well as within days 8 and 9 (Fig. 6D; three-way repeated measures ANOVA, $F_{1,23}=12.79$, $p<0.01$). The reduction in escape latency in the second trial compared with that in the first trial reflects the mouse's ability to acquire memory of the platform location based on a single exposure against interference by memories of other platform locations acquired in previous days. We found a significant difference between genotypes in the reduction in the escape latency in the second trial compared with that in the first (Fig. 6E; ANOVA $F_{1,23}=7.28$, $p<0.05$), showing that Rac1 mutants were impaired in their ability to acquire a memory of the platform location compared to littermate controls.

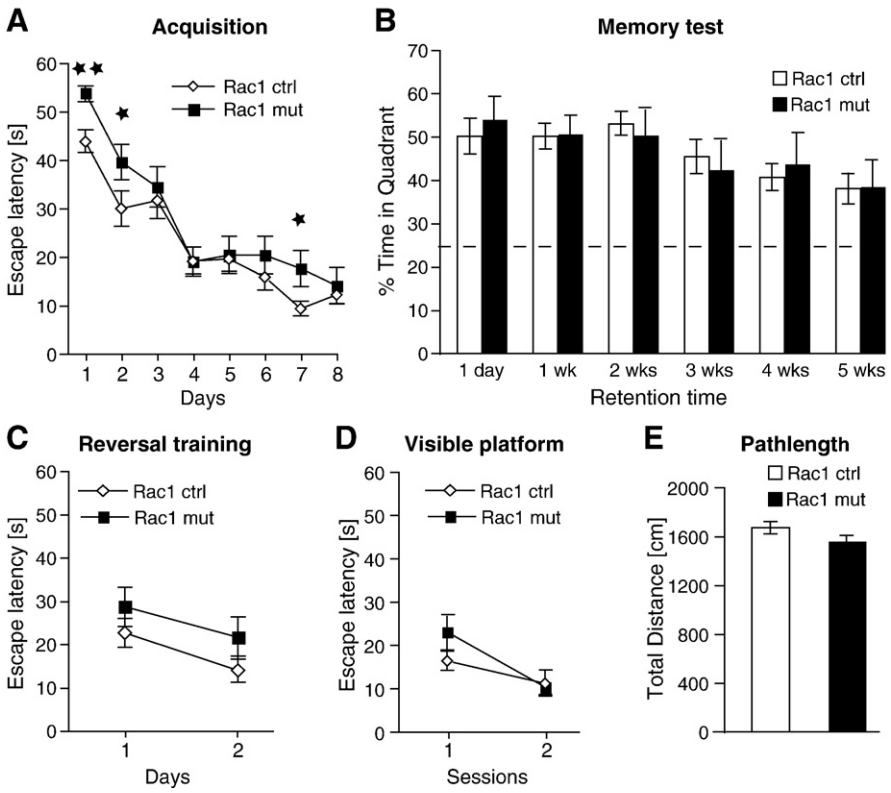

Fig. 5. Loss of Rac1 impairs spatial learning (A) Mutant and control mice were trained on the Morris water maze for 8 days with 6 training trials per day. Mean escape latencies across days (average of 6 sessions per day) are shown. Rac1 mutants ($n=11$) had significantly higher escape latencies than control animals ($n=15$) on days 1, 2 and 7 (overall genotype effect, two-way repeated measures ANOVA, $F_{1,24}=4.66$, $p<0.05$; ANOVA with Newman–Keuls post hoc test, $^*p<0.05$). (B) Mutant mice showed normal spatial memory compared to controls. Probe trials were performed 1 day, 1, 2, 3, 4 and 5 weeks after the training. The dashed line indicates chance level (25%). (C) Reversal training assessed after the last probe trial in the reference memory task revealed no significant differences in escape latency between Rac1 mutants ($n=11$) and control animals ($n=15$) (ANOVA with Newman–Keuls post hoc test, $^*p>0.1$). (D) Mutant mice showed normal learning on the cued version of the Morris water maze. (E) No differences were detected in the total distance swam within the one-minute probe trials between control and mutant mice.

Hippocampus-dependent learning is accompanied by an increase in the density of dendritic spines on hippocampal neurons, which can be mediated by an upregulation of brain-derived neurotrophic factor (BDNF) expression (Hall et al., 2000; Tyler and Pozzo-Miller, 2003). As expected, the density of PSD-95$^+$ puncta in EGFP$^+$ Rac1-deficient neurons increased significantly in both the CA1 region and GCL of mutant animals trained on the DMP task compared to corresponding naïve animals (ANOVA, CA1, $F_{(1,9)}=15.83$, $p<0.001$; DG, $F_{(1,9)}=6.52$, $p<0.05$). However, the density of PSD-95$^+$ puncta was significantly lower in these hippocampal regions in trained mutant mice compared to trained controls (Fig. 6G, Fig. S2D). These data provide an anatomical correlate of the decreased learning exhibited by Rac1-deficient mice.

Discussion

The aim of this study was to investigate the role of Rac1 in synaptic plasticity and cognition. The conditional ablation of Rac1 in excitatory neurons of the forebrain revealed that hippocampal neurons had significantly fewer PSD-95$^+$ clusters, but larger spines relative to control mice. These abnormalities correlated with impaired LTP and functional deficits in spatial learning and working/episodic-like memory.

The roles of Rac1 in neurons of the hippocampus in vivo

Studies of the role of Rac1 in spine morphogenesis *in vivo* have suggested that Rac1 plays an important role in regulating the size and density of spines in cerebellar Purkinje cells (Luo et al., 1996). These studies showed that transgenic mice overexpressing a constitutively active form of Rac1 (RacV12) have smaller spines with higher density in comparison to control mice. However, overexpression of this construct in slice culture produced conflicting results: RacV12 induced an enlargement of spine heads shortly after transfection (Tashiro et al., 2000), whereas the spines of neurons overexpressing a dominant-negative form of Rac1, RacN17, were longer and narrower than in controls (Tashiro and Yuste, 2004). Despite these contradictory results, it has been suggested that Rac1 is involved in spine maturation and induces the enlargement of spine heads (Tashiro and Yuste, 2008).

Here we demonstrate that loss of Rac1 in the hippocampus *in vivo* increases spine head size and reduces the number of PSD-95$^+$ clusters. Our data shows that the formation of new PSD-95$^+$ clusters in Rac1 mutants does occur in response to learning (Rac1 mutants trained in the DMP task had significantly increased PSD-95 density relative to Rac1 untrained mutants, Fig. 3B); however, fewer PSD-95$^+$ spines were present in the mutants vs. controls after training (Fig. 6G). A reduction of spine density has also been observed in RacN17-transfected neurons (Nakayama et al., 2000; Tashiro and Yuste, 2004) in culture, and time-lapse analysis revealed that the reduced density is due to a decrease in spine stability and not due to changes in spine retraction or formation (Tashiro and Yuste, 2004). In combination, this strongly suggests that Rac1 ablation *in vivo* decreases stability of new PSD-95$^+$ spines formed during learning leading to a net reduction in the normal learning-induced increase in PSD-95$^+$ clusters. The initial increase must be independent of Rac1 in the mutant mice and might be achieved through the activation of the Rho GTPases Cdc42. Recent studies have indicated a role for Cdc42 in dendritic morphogenesis in *Drosophila* and in learning-related synaptic growth in *Aplysia* sensory neurons (Scott et al., 2003; Udo et al., 2005). Furthermore, dominant-negative overexpression of Cdc42 and knockdown of Cdc42 by RNAi

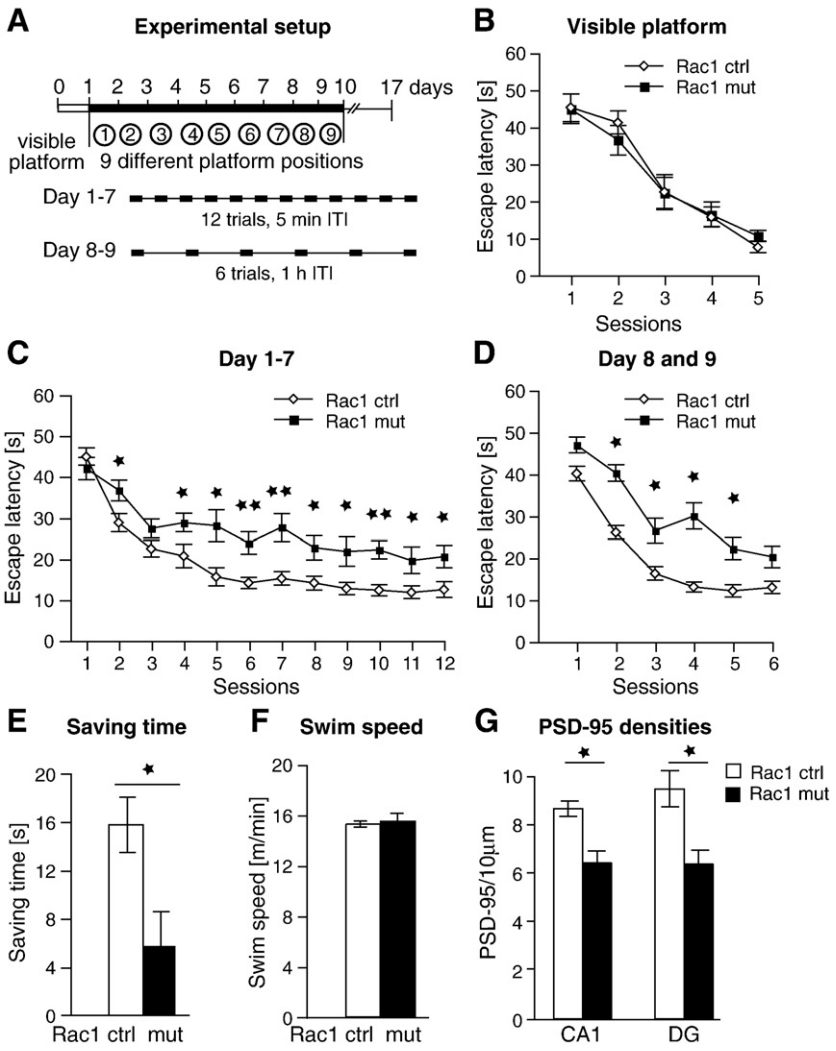

Fig. 6. Loss of Rac1 impairs working memory. (A) Experimental setup of the delayed matching-to-place (DMP) paradigm. After one day training in the cued version of the Morris water maze, animals were trained for 9 days in the DMP task, learning 9 different platform locations (one per day). On days 1–7, the interval between training trials was 5 min; on days 8–9, the interval was increased to 1 h with 6 trials a day. (B) Visible platform training on day 0 of the DMP task. No differences in visual acuity were observed between control ($n=12$) and mutant mice ($n=13$). (C) Latencies of the 12 sessions per day averaged from days 1–7. Rac1 mutant mice displayed impaired working memory (controls, $n=12$; mutants, $n=13$;three-way repeated measures ANOVA for overall genotype effect, $F_{1,23}=9.96$, $p<0.01$ and ANOVA with Newman–Keuls post hoc test $^{*}p<0.05$, $^{**}p<0.01$). (D) Latencies of the 6 trials per day (1 h ITI) averaged from days 8 and 9. Control mice found the platform faster than mutant mice (controls, $n=12$; mutants, $n=13$; three-way repeated measures ANOVA for overall genotype effect, $F_{1,23}=12.78$, $p<0.01$ and ANOVA with Newman–Keuls post hoc test, $^{*}p<0.05$, $^{**}p<0.01$). (E) Mutant mice showed a significant decrease in the time saved (reduction in latencies) between the first and second trials of each day, averaged from all days (ANOVA, $F_{1,23}=7.28$, $^{*}p<0.05$). (F) No difference was observed in swim speed between controls and mutants (ANOVA $p>0.05$). (G) PSD-95^{+} densities were measured in both CA1 and GCL. Rac1 mutants showed reduced number of PSD-95^{+} clusters compared to controls ($n=4$ for all groups; ANOVA, CA1, $F_{1,6}=6.3$; DG, $F_{1,6}=6.0$, in both cases $^{*}p<0.05$).

significantly decreased the number of spines and PSD-95^{+} synapses (Irie and Yamaguchi, 2002; Wegner et al., 2008) in hippocampal neurons. We speculate here that Cdc42 activity regulates the formation of new spines and synapses while Rac1 may play a larger role in stabilizing newly formed spines.

The role of Rac1 in synaptic plasticity

Activity-dependent changes in synapse structure and function rely in part on rearrangements of the actin cytoskeleton; hence, actin and its regulators are likely to play key roles in activity-dependent plasticity. Indeed, LTP-induced accumulation of actin in spines is required for the maintenance of LTP (Fukazawa et al., 2003). Furthermore, activity-dependent spine enlargement goes hand in hand with synapse stabilization and functional strengthening of synapses and is associated with increased AMPAR levels at the postsynaptic membrane (Kasai et al., 2003; Matsuzaki et al., 2004). Induction of chemical LTP is associated with elevated Rac1 and JNK kinase activity. Once activated, this signaling pathway leads to the phosphorylation of ser-295 of PSD-95, which enhances the ability of PSD-95 to accumulate in the PSD and to recruit surface AMPA receptors, thereby potentiating excitatory postsynaptic currents (Kim et al., 2007). Thus Rac1 activity is important for the regulation of both actin dynamics and AMPA receptor clustering during synapse maturation (Hall, 1998, 2005; Wiens et al., 2005). It is therefore not surprising that loss of Rac1 in excitatory neurons in the hippocampus results in impaired LTP. We have not directly examined the level of AMPA receptors located on postsynaptic densities; however the fact that Rac1 mutants did not display any changes in the basal synaptic transmission (Figs. 4C and D) suggests that the net function of AMPA receptors in the mutant mice might not be altered.

The observed decrease in P-PAK in Rac1 mutants (Fig. 2) suggests that actin polymerization, through phosphorylation of LIM kinase and inactivation of cofilin (Edwards et al., 1999), may be affected in the mutants, which then would impair activity-dependent spine enlargement. A recent study revealed that overexpression of dominant-

negative PAK (which inhibits all three PAK isoforms) in the forebrain of transgenic mice leads to reduced spine density and increased size of spine heads (Hayashi et al., 2004). These mice also exhibit enhanced LTP and decreased LTD in cortical neurons. However, hippocampal neurons failed to show altered synaptic plasticity or spine morphology, probably because PAK inhibition did not reach a critical threshold in the hippocampus (Hayashi et al., 2004). In contrast to the results from cortex but consistent with our own data, Asrar et al. (2009) showed that the disruption of PAK1 in the hippocampus impairs LTP at CA1 synapses. Collectively these data suggest that decreases in PAK activity in cortical and hippocampal neurons have differential effects on LTP and synaptic morphology. One possible explanation for this discrepancy could be that changes in spine size and densities have distinct effects on synaptic plasticity in the cortex and hippocampus. It appears that the decrease in the number of PSD-95$^+$ spines in CA1 neurons of Rac1 mutants (Fig. 3) cannot be compensated by the increase in spine size and that the overall reduced number of PSD-95$^+$ spines (Fig. S2) leads to an overall decrease in LTP.

Rac1 may also play an important role in regulating a neuron's ability to undergo LTP via other signaling pathways that lead to alterations in gene transcription. Rac1 regulates transcription through the p38 mitogen-activated protein kinase (p38-MAPK) and Erk1/2 signaling cascades (Coso et al., 1995; Eblen et al., 2002; Li et al., 2001; Loucks et al., 2006; Minden et al., 1995). Proteins in the MAPK/ERK pathway, as well as two downstream transcription factors, Elk-1 and CREB, are rapidly phosphorylated after the induction of LTP; inhibition of the MAPK/ERK pathway blocks LTP-induced phosphorylation of Elk-1 and CREB and results in a rapidly decaying LTP (Davis et al., 2000; English and Sweatt, 1997). Thus, the loss of Rac1 could impair LTP through resulting alterations in transcriptional control, actin-dependent changes, or both. Future studies employing genetic or pharmacological perturbations may provide mechanistic insight into the mechanisms by which Rac1 regulates synaptic plasticity.

The role of Rac1 in learning and memory

Transgenic mice expressing a dominant-negative form of PAK exhibit long-term memory deficits in the Morris water maze test (Hayashi et al., 2004), suggesting a link between memory storage and decreased PAK activity. However, learning was not affected in these mice, probably because PAK activity was not significantly altered in the hippocampus. The genetic disruption of WAVE1, another Rac1-specific downstream target that acts as a scaffolding protein to relay signals from Rac1 to the Arp2/3 complex and thus directs actin reorganization, has been correlated with learning deficits in the Morris water maze test (Soderling et al., 2003). However, the WAVE1-deficient mice also show severe sensory motor deficits, resulting in slower swim speed in the water maze and have increased anxiety, which has made interpreting the learning impairments difficult.

In a recent study, Diana et al. (2007) have suggested that activation of Rho GTPases can improve learning and memory. In this study, the bacterial toxin cytotoxic necrotizing factor 1 (CNF1) was injected intracerebroventricularly 10 days before behavioral testing. CNF1 deamidates glutamine 63/61 of the Rho family members RhoA, Rac1 and Cdc42 (Flatau et al., 1997; Schmidt et al., 1997), thus abrogating their GTPase activity and leading to a state of constitutive activation of the Rho GTPases; at the same time CNF1 rapidly conveys RhoGTPases to the ubiquitin-mediated proteasomal degradation pathway (Doye et al., 2002; Lerm et al., 2002). Ten days after the CNF1 injection, mice showed a slight improvement in learning in the Morris water maze, which the authors attributed to an elevation Rac1 activity. However, CNF1 confers a variety of additional activities besides the transient activation of Rho GTPases, such as the release of pro-inflammatory cytokines or the activation of transcription factor NF-kB (Travaglione et al., 2008); thus it has been difficult to ascertain whether changes in Rac1 activity alone are important for learning and memory.

Here we have demonstrated that loss of Rac1 indeed impairs learning in the reference memory task of the Morris water maze, without affecting long-term memory (Fig. 5). Memories are believed to be initially and temporarily stored in the hippocampus and later transferred to the cortex for persistent storage during a process named system consolidation. The fact that long-term memory was not affected in the mutants suggests that Rac1 might not play a major role in memory consolidation. However, we have not ascertained directly whether loss of Rac1 in the cortex causes structural or molecular changes in mutant neurons.

In addition to the learning impairments, we observed more robust deficits in working/episodic-like memory in the delayed matching-to-place (DMP) task in the Rac1 mutants. Previous studies have shown that performance in the DMP task is disrupted completely by hippocampal lesions and is sensitive to blockage of the NMDA receptor-dependent synaptic plasticity (Steele and Morris, 1999). Intra-hippocampal infusion of the NMDA receptor antagonist D-AP5 causes delay-dependent memory impairments at the second trial of each day, suggesting that animals encode the information about platform positions at the end of each trial using an NMDA receptor-dependent mechanism. Furthermore, conditional ablation of the NMDA receptor 1 (NR1) in CA3 neurons impairs learning on the DMP task, demonstrating the NMDAR-mediated signaling is required for rapid hippocampal encoding of novel information and fast learning of one-time experience (Nakazawa et al., 2003).

Rac1 is activated downstream of the NMDA receptor by the Rac1-specific GEF TIAM1, and by the Cdc42- and Rac1-specific GEFs kalirin-7 and βPIX (Saneyoshi et al., 2008; Tolias et al., 2005; Xie et al., 2007). Recent work shows that a single training trial of associative fear conditioning results in rapid Rac1 and PAK activation and the membrane translocation of Rac1, all of which can be blocked by the NMDA receptor channel blocker MK801 prior to training. This suggests that NMDA receptor activation during learning is responsible for changes in Rac1 activity and PAK activity after contextual fear conditioning. Thus, it is conceivable that loss of Rac1 in the hippocampus could impair the encoding of the fast one-trial learning in the DMP task. Indeed, we observed significant decrease in the time saved between the first and second trials of each day (Fig. 6E) in Rac1 mutants, suggesting that these mice cannot learn the new location of the platform as quickly as controls, and/or that they are less able to suppress the interfering memory of the previous platform location.

Taken together, our data demonstrate that Rac1 activation is important for rapid encoding of information and loss of Rac1 impairs the acquisition of spatial memory without affecting spatial long-term memory. Future experiments studying downstream effectors of Rac1 activity will be necessary to understand how Rac1 contributes to the rapid acquisition of new information *in vivo*.

Experimental methods

Mice

Mice bearing a conditional allele of Rac1 (Chrostek et al., 2006) were crossed with animals carrying CamKIIα-Cre (line 2834, Schweizer et al., 2003). To generate Rac1 null animals, mice hemizygous for the Cre transgene and heterozygous for the floxed allele (Cre$^+$; Rac1$^{lox/wt}$) were crossed to mice that were homozygous for the floxed allele but lacked Cre (Rac1$^{lox/lox}$; Cre$^-$) to produce littermates that were either Cre$^+$ or Cre$^-$ and either homozygous (lox/lox) or heterozygous (lox/wt) for the target alleles. To visualize Cre-mediated recombination, mice carried either the Z/EG (Novak et al., 2000) or the R26R (Soriano, 1999) reporter allele. For all experiments, male mutant mice (Cre$^+$; Rac1$^{lox/lox}$) and their control littermates (Cre$^-$; Rac1$^{lox/lox}$ or Cre$^+$; Rac1$^{lox/wt}$) were 2–6 months old. The mice were housed under standard housing conditions in a 12-h (07:00–19:00) light–dark colony room at 22 °C with freely available

food and water in accordance with the policies set forth by the Stanford Animal Care and Use Committee.

Tissue preparation and histology

Mice were deeply anesthetized with ketamine/xylazine (100 mg/kg and 7 mg/kg, respectively), then transcardially perfused (cold saline followed by 4% cold paraformaldehyde in 0.1 M phosphate buffer), and brains were collected for immunohistochemistry. All brains were post-fixed overnight in 4% paraformaldehyde at 4 °C, then cryoprotected in 30% sucrose and stored at 4 °C. Serial coronal sections (40 μm) were cut through the entire hippocampus on a dry-ice-cooled block on a sliding microtome (Leica). The sections were stored at −20 °C in cryoprotectant with 25% ethylene glycol, 25% glycerin and 0.1 M phosphate buffer.

Sections were stained with free-floating immunohistochemistry and incubated in tris-buffered saline (TBS) with 0.3% Triton X-100 and 1% normal donkey serum at 4 °C overnight containing the following primary antibodies: mouse anti-β-galactosidase (1:100, Molecular Probes), rabbit or mouse anti-GFP (1:500, Molecular Probes), rabbit anti-Rac1 (1:100, Santa Cruz) and goat anti-P-γPAK (1:500, Santa Cruz). Species-specific fluorescent secondary antibodies from donkey conjugated with FITC, Cy3, or Cy5 were obtained from Jackson Laboratories and all used at 1:500. Fluorescent signals were detected using a spectral confocal microscope (Zeiss LSM 510 Meta). Split panel and *z*-axis analysis were used for all counting. All counts were performed using multi-channel configuration with a 40× objective and electronic zoom of 2.

Electron microscopy and PSD-95 density

For the analysis of PSD-95 density, 40 μm floating sections (see above) were incubated in blocking buffer (200 mM NaCl2, 60 mM Tris-Base, 1% BSA, 100 mM L-Lysine, pH = 7.4) containing 50% normal donkey serum and 1% triton for 3 h at room temperature and then incubated in the same buffer with 0.3% triton and 1% donkey serum containing anti-rabbit PSD-95 (1:200, Zymed) and anti-mouse EGFP (1:500, Molecular Probes) at 4 °C overnight. For quantification, EGFP-positive basal dendrites of CA1 neurons (25–100 mm from the cell body) were analyzed. Serial confocal images (Z steps of 0.5 μm) were taken of Cy3 (detecting PSD-95) and FITC (detecting EGFP-labeled dendrites) fluorescence with a 63× objective and a digital zoom factor of 2. The number of PSD-95 clusters per dendrite was counted using LSM Image Browser software from Zeiss.

For electron microscopy, 40 μm floating sections were stained for EGFP using peroxidase-DAB histochemical staining using ABC kit (Vector) amplification of the HRP signal. After developing with DAB and NiCl for 10 min the sections were post-fixed with osmium tetroxide for 1 hr at 4 °C, then washed for 15 min in water and stained with uranyl acetate for 2 h. Dehydration and infiltration with resin was performed by using standard protocols. One μm thick sections were cut and stained with 1% toluidine blue to guide further trimming to isolate regions of interest (stratum radiatum of the hippocampus). Post-embedding staining of the ultra-microtome sections (90 nm) mounted on grids was not performed to maintain contrast between labeled and unlabeled membranes. Electron micrographs were produced using a JoeL 1230 transmission electron microscope and Gatan 967 CCD imaging software. Images were further analyzed using ImageJ.

Electrophysiological recordings

Mice were anaesthetized with isoflurane and then decapitated. Heads were immediately immersed in ice-cold artificial cerebrospinal fluid (aCSF) for at least 2 min before brain extraction. Acute slices (400 μm thick) were prepared with a vibratome (Leica VT 1000S) in aCSF. Sections were incubated in aCSF at 34 °C for 20 min, then kept at room temperature for at least 1 h before recording. Recording was performed in an interface chamber continuously flowed with aCSF at 1.1 ml/min. A monopolar electrode was placed in the Schaffer collaterals and stimulation was applied at 0.033 Hz with stimulus intensity ranging from 20–80 μA, yielding evoked field excitatory postsynaptic potentials (fEPSPs) of 0.2–0.5 V. fEPSPs were recorded in the stratum radiatum using a borosilicate micropipette filled with aCSF. The signal was amplified with an AXOPATCH 200B amplifier (Axon Instruments), digitized by a Digidata 1200 interface (AxonInstruments) and sampled at 10 kHz with Clampex 8.2 (AxonInstruments). aCSF was composed of: 119 mM NaCl, 11 mM D-glucose, 1.3 mM $MgCl_2 \cdot 6H2O$, 1.3 mM NaH_2PO4, 2.5 mM KCl, 2.5 mM $CaCl_2$, 26 mM $NaHCO_3$, gazed with O_2/CO_2 (95/5%) at least 20 min before use and throughout the experiment. Baseline was recorded for a minimum of 20 min or until stable. Plasticity was then induced by stimulation with 100 Hz for 3 trains of 1 s tetanus separated by 20 s. Data was analyzed by measuring the slope of individual fEPSPs at 1–1.5 ms after the stimulus pulse by linear fitting using Clampfit (Axon Instruments). The experimenter was blind to the mouse genotype.

Behavior

Reference memory

For all behavioral tasks, mutant and control littermates (males, 3–5 months old) were used. The water maze consisted of a circular black tank (170 cm diameter, 43 cm deep) filled with water (23–25 °C) containing non-toxic tempera paint (Rich Art Color Co. Inc, Nrothvale, CA) to obscure the submerged platform. At the start of each trial, the mouse was gently placed into the water with its head facing the wall of the pool. The start location varied semi-randomly between trials (3 different starting locations spaced evenly around the pool). If a mouse did not find the platform (13 cm diameter, 29 cm height) within a 60-s trial, it was placed onto the platform by the experimenter, stayed there for 15 s and then removed to a warmed home cage. Data (swim speed, path length, location) were collected using a video tracking system (Videotrack Automated Behavioral Analysis Stystem, Viewpoint Life Sciences Inc, France). During the visible platform training, the platform location was indicated by a flag rising above the water line and visible from all areas within the pool. In hidden platform training, the platform location was not marked and thus could only be discerned using extra-maze cues.

For the reference memory task, training consisted of 6 trials per day with inter-trial interval (ITI) of 30–50 min for 8 days. For probe trials, the platform was removed from the maze and the animals were allowed a 60-s search. The same groups of mice were successively tested on each probe trial. The time (%) spent in each quadrant of the maze was recorded. Animals were left on the platform for 15 s after each training trial and each probe trial.

Delayed matching-to-place task

For training in the delayed matching-to-place (DMP), the platform was moved to a new location each day, but within each day the platform location remained constant. There were 9 possible platform locations, each used only once. The DMP training consisted of 12 training trials per day with 5 min ITI on days 1–7 and 6 training trials 1 h apart for days 8 and 9. For the analysis, 12 sessions were averaged across days 1–7 and the 6 trials were averages across days 8 and 9. The experimenter was blind to genotype for all behavioral tests.

Data analysis

Statistical analysis was performed using Statistica software (StatSoft Inc. Tulsa, OK). In repeated measures comparisons conducted for electrophysiological and behavioral analyses, dependent variables were analyzed using analysis of variance (ANOVA) with

genotype as the between-subject factor, and session as the within-subject factor. Statistically significant effects revealed by ANOVA were explored using Newman–Keuls post hoc test. Means ± SEM are presented.

Acknowledgments

We would like to thank John Perrino for his help regarding electron microscopy. This work was supported in part by funding from the NIH (NS045113, MH071472) the California Institute of Regenerative Medicine (RC1-00134), and the Kinetics Foundation.

Appendix A. Supplementary data

Supplementary data associated with this article can be found, in the online version, at doi:10.1016/j.mcn.2009.04.005.

References

Asrar, S., Meng, Y., Zhou, Z., Todorovski, Z., Huang, W.W., Jia, Z., 2009. Regulation of hippocampal long-term potentiation by p21-activated protein kinase 1 (PAK1). Neuropharmacology 56, 73–80.
Bamburg, J.R., 1999. Proteins of the ADF/cofilin family: essential regulators of actin dynamics. Annu. Rev. Cell Dev. Biol. 15, 185–230.
Bokoch, G.M., 2003. Biology of the p21-activated kinases. Annu. Rev. Biochem. 72, 743–781.
Bonhoeffer, T., Yuste, R., 2002. Spine motility. Phenomenology, mechanisms, and function. Neuron 35, 1019–1027.
Calabrese, B., Wilson, M.S., Halpain, S., 2006. Development and regulation of dendritic spine synapses. Physiology (Bethesda). 21, 38–47.
Chrostek, A., Wu, X., Quondamatteo, F., Hu, R., Sanecka, A., Niemann, C., Langbein, L., Haase, I., Brakebusch, C., 2006. Rac1 is crucial for hair follicle integrity but is not essential for maintenance of the epidermis. Mol. Cell. Biol. 26, 6957–6970.
Coso, O.A., Chiariello, M., Yu, J.C., Teramoto, H., Crespo, P., Xu, N., Miki, T., Gutkind, J.S., 1995. The small GTP-binding proteins Rac1 and Cdc42 regulate the activity of the JNK/SAPK signaling pathway. Cell 81, 1137–1146.
Davis, S., Vanhoutte, P., Pages, C., Caboche, J., Laroche, S., 2000. The MAPK/ERK cascade targets both Elk-1 and cAMP response element-binding protein to control long-term potentiation-dependent gene expression in the dentate gyrus *in vivo*. J. Neurosci. 20, 4563–4572.
Diana, G., Valentini, G., Travaglione, S., Falzano, L., Pieri, M., Zona, C., Meschini, S., Fabbri, A., Fiorentini, C., 2007. Enhancement of learning and memory after activation of cerebral Rho GTPases. Proc. Natl. Acad. Sci. U. S. A. 104, 636–641.
Dillon, C., Goda, Y., 2005. The actin cytoskeleton: integrating form and function at the synapse. Annu. Rev. Neurosci. 28, 25–55.
Doye, A., Mettouchi, A., Bossis, G., Clement, R., Buisson-Touati, C., Flatau, G., Gagnoux, L., Piechaczyk, M., Boquet, P., Lemichez, E., 2002. CNF1 exploits the ubiquitin-proteasome machinery to restrict Rho GTPase activation for bacterial host cell invasion. Cell 111, 553–564.
Eblen, S.T., Slack, J.K., Weber, M.J., Catling, A.D., 2002. Rac-PAK signaling stimulates extracellular signal-regulated kinase (ERK) activation by regulating formation of MEK1-ERK complexes. Mol. Cell. Biol. 22, 6023–6033.
Edwards, D.C., Sanders, L.C., Bokoch, G.M., Gill, G.N., 1999. Activation of LIM-kinase by Pak1 couples Rac/Cdc42 GTPase signalling to actin cytoskeletal dynamics. Nat. Cell Biol. 1, 253–259.
English, J.D., Sweatt, J.D., 1997. A requirement for the mitogen-activated protein kinase cascade in hippocampal long term potentiation. J. Biol. Chem. 272, 19103–19106.
Flatau, G., Lemichez, E., Gauthier, M., Chardin, P., Paris, S., Fiorentini, C., Boquet, P., 1997. Toxin-induced activation of the G protein p21 Rho by deamidation of glutamine. Nature 387, 729–733.
Fukazawa, Y., Saitoh, Y., Ozawa, F., Ohta, Y., Mizuno, K., Inokuchi, K., 2003. Hippocampal LTP is accompanied by enhanced F-actin content within the dendritic spine that is essential for late LTP maintenance *in vivo*. Neuron 38, 447–460.
Geinisman, Y., 2000. Structural synaptic modifications associated with hippocampal LTP and behavioral learning. Cereb. Cortex 10, 952–962.
Hall, A., 1998. Rho GTPases and the actin cytoskeleton. Science 279, 509–514.
Hall, A., 2005. Rho GTPases and the control of cell behaviour. Biochem. Soc. Trans. 33, 891–895.
Hall, J., Thomas, K.L., Everitt, B.J., 2000. Rapid and selective induction of BDNF expression in the hippocampus during contextual learning. Nat. Neurosci. 3, 533–535.
Harris, K.M., Fiala, J.C., Ostroff, L., 2003. Structural changes at dendritic spine synapses during long-term potentiation. Philos. Trans. R Soc. Lond. B Biol. Sci. 358, 745–748.
Hayashi, M.L., Choi, S.Y., Rao, B.S., Jung, H.Y., Lee, H.K., Zhang, D., Chattarji, S., Kirkwood, A., Tonegawa, S., 2004. Altered cortical synaptic morphology and impaired memory consolidation in forebrain-specific dominant-negative PAK transgenic mice. Neuron 42, 773–787.
Irie, F., Yamaguchi, Y., 2002. EphB receptors regulate dendritic spine development via intersectin, Cdc42 and N-WASP. Nat. Neurosci. 5, 1117–1118.
Kasai, H., Matsuzaki, M., Noguchi, J., Yasumatsu, N., Nakahara, H., 2003. Structure–stability–function relationships of dendritic spines. Trends Neurosci. 26, 360–368.
Kim, M.J., Futai, K., Jo, J., Hayashi, Y., Cho, K., Sheng, M., 2007. Synaptic accumulation of PSD-95 and synaptic function regulated by phosphorylation of serine-295 of PSD-95. Neuron 56, 488–502.
Lerm, M., Pop, M., Fritz, G., Aktories, K., Schmidt, G., 2002. Proteasomal degradation of cytotoxic necrotizing factor 1-activated rac. Infect. Immun. 70, 4053–4058.
Li, W., Chong, H., Guan, K.L., 2001. Function of the Rho family GTPases in Ras-stimulated Raf activation. J. Biol. Chem. 276, 34728–34737.
Loucks, F.A., Le, S.S., Zimmermann, A.K., Ryan, K.R., Barth, H., Aktories, K., Linseman, D.A., 2006. Rho family GTPase inhibition reveals opposing effects of mitogen-activated protein kinase kinase/extracellular signal-regulated kinase and Janus kinase/signal transducer and activator of transcription signaling cascades on neuronal survival. J. Neurochem. 97, 957–967.
Luo, L., Hensch, T.K., Ackerman, L., Barbel, S., Jan, L.Y., Jan, Y.N., 1996. Differential effects of the Rac GTPase on Purkinje cell axons and dendritic trunks and spines. Nature 379, 837–840.
Matsuzaki, M., Honkura, N., Ellis-Davies, G.C., Kasai, H., 2004. Structural basis of long-term potentiation in single dendritic spines. Nature 429, 761–766.
Minden, A., Lin, A., Claret, F.X., Abo, A., Karin, M., 1995. Selective activation of the JNK signaling cascade and c-Jun transcriptional activity by the small GTPases Rac and Cdc42Hs. Cell 81, 1147–1157.
Miyamoto, Y., Yamauchi, J., Tanoue, A., Wu, C., Mobley, W.C., 2006. TrkB binds and tyrosine-phosphorylates Tiam1, leading to activation of Rac1 and induction of changes in cellular morphology. Proc. Natl. Acad. Sci. U. S. A. 103, 10444–10449.
Morris, R.G., Garrud, P., Rawlins, J.N., O'Keefe, J., 1982. Place navigation impaired in rats with hippocampal lesions. Nature 297, 681–683.
Munro, P., Flatau, G., Doye, A., Boyer, L., Oregioni, O., Mege, J.L., Landraud, L., Lemichez, E., 2004. Activation and proteasomal degradation of rho GTPases by cytotoxic necrotizing factor-1 elicit a controlled inflammatory response. J. Biol. Chem. 279, 35849–35857.
Nakayama, A.Y., Harms, M.B., Luo, L., 2000. Small GTPases Rac and Rho in the maintenance of dendritic spines and branches in hippocampal pyramidal neurons. J. Neurosci. 20, 5329–5338.
Nakazawa, K., Sun, L.D., Quirk, M.C., Rondi-Reig, L., Wilson, M.A., Tonegawa, S., 2003. Hippocampal CA3 NMDA receptors are crucial for memory acquisition of one-time experience. Neuron 38, 305–315.
Novak, A., Guo, C., Yang, W., Nagy, A., Lobe, C.G., 2000. Z/EG, a double reporter mouse line that expresses enhanced green fluorescent protein upon Cre-mediated excision. Genesis 28, 147–155.
Penzes, P., Beeser, A., Chernoff, J., Schiller, M.R., Eipper, B.A., Mains, R.E., Huganir, R.L., 2003. Rapid induction of dendritic spine morphogenesis by trans-synaptic ephrinB-EphB receptor activation of the Rho-GEF kalirin. Neuron 37, 263–274.
Saneyoshi, T., Wayman, G., Fortin, D., Davare, M., Hoshi, N., Nozaki, N., Natsume, T., Soderling, T.R., 2008. Activity-dependent synaptogenesis: regulation by a CaM-kinase kinase/CaM-kinase I/betaPIX signaling complex. Neuron 57, 94–107.
Schmidt, G., Sehr, P., Wilm, M., Selzer, J., Mann, M., Aktories, K., 1997. Gln 63 of Rho is deamidated by Escherichia coli cytotoxic necrotizing factor-1. Nature 387, 725–729.
Schweizer, C., Balsiger, S., Bluethmann, H., Mansuy, I.M., Fritschy, J.M., Mohler, H., Luscher, B., 2003. The gamma 2 subunit of GABA(A) receptors is required for maintenance of receptors at mature synapses. Mol. Cell. Neurosci. 24, 442–450.
Scott, E.K., Reuter, J.E., Luo, L., 2003. Small GTPase Cdc42 is required for multiple aspects of dendritic morphogenesis. J. Neurosci. 23, 3118–3123.
Soderling, S.H., Langeberg, L.K., Soderling, J.A., Davee, S.M., Simerly, R., Raber, J., Scott, J.D., 2003. Loss of WAVE-1 causes sensorimotor retardation and reduced learning and memory in mice. Proc. Natl. Acad. Sci. U. S. A. 100, 1723–1728.
Soriano, P., 1999. Generalized lacZ expression with the ROSA26 Cre reporter strain. Nat. Genet. 21, 70–71.
Stanyon, C.A., Bernard, O., 1999. LIM-kinase1. Int. J. Biochem. Cell Biol. 31, 389–394.
Steele, R.J., Morris, R.G., 1999. Delay-dependent impairment of a matching-to-place task with chronic and intrahippocampal infusion of the NMDA-antagonist D-AP5. Hippocampus 9, 118–136.
Tashiro, A., Minden, A., Yuste, R., 2000. Regulation of dendritic spine morphology by the rho family of small GTPases: antagonistic roles of Rac and Rho. Cereb. Cortex 10, 927–938.
Tashiro, A., Yuste, R., 2004. Regulation of dendritic spine motility and stability by Rac1 and Rho kinase: evidence for two forms of spine motility. Mol. Cell. Neurosci. 26, 429–440.
Tashiro, A., Yuste, R., 2008. Role of Rho GTPases in the morphogenesis and motility of dendritic spines. Methods Enzymol. 439, 285–302.
Tolias, K.F., Bikoff, J.B., Burette, A., Paradis, S., Harrar, D., Tavazoie, S., Weinberg, R.J., Greenberg, M.E., 2005. The Rac1-GEF Tiam1 couples the NMDA receptor to the activity-dependent development of dendritic arbors and spines. Neuron 45, 525–538.
Tolias, K.F., Bikoff, J.B., Kane, C.G., Tolias, C.S., Hu, L., Greenberg, M.E., 2007. The Rac1 guanine nucleotide exchange factor Tiam1 mediates EphB receptor-dependent dendritic spine development. Proc. Natl. Acad. Sci. U. S. A. 104, 7265–7270.
Travaglione, S., Fabbri, A., Fiorentini, C., 2008. The Rho-activating CNF1 toxin from pathogenic E. coli: a risk factor for human cancer development? Infect. Agent Cancer 3, 4.
Tyler, W.J., Pozzo-Miller, L., 2003. Miniature synaptic transmission and BDNF modulate dendritic spine growth and form in rat CA1 neurones. J. Physiol. 553, 497–509.
Udo, H., Jin, I., Kim, J.H., Li, H.L., Youn, T., Hawkins, R.D., Kandel, E.R., Bailey, C.H., 2005. Serotonin-induced regulation of the actin network for learning-related synaptic growth requires Cdc42, N-WASP, and PAK in Aplysia sensory neurons. Neuron 45, 887–901.
van Galen, E.J., Ramakers, G.J., 2005. Rho proteins, mental retardation and the neurobiological basis of intelligence. Prog. Brain Res. 147, 295–317.

Wegner, A.M., Nebhan, C.A., Hu, L., Majumdar, D., Meier, K.M., Weaver, A.M., Webb, D.J., 2008. N-wasp and the arp2/3 complex are critical regulators of actin in the development of dendritic spines and synapses. J. Biol. Chem. 283, 15912–15920.
Wiens, K.M., Lin, H., Liao, D., 2005. Rac1 induces the clustering of AMPA receptors during spinogenesis. J. Neurosci. 25, 10627–10636.
Xie, Z., Srivastava, D.P., Photowala, H., Kai, L., Cahill, M.E., Woolfrey, K.M., Shum, C.Y., Surmeier, D.J., Penzes, P., 2007. Kalirin-7 controls activity-dependent structural and functional plasticity of dendritic spines. Neuron 56, 640–656.
Zhang, H., Webb, D.J., Asmussen, H., Horwitz, A.F., 2003. Synapse formation is regulated by the signaling adaptor GIT1. J. Cell Biol. 161, 131–142.